Journal of Photochemistry and Photobiology A: Chemistry 223 (2011) 57–64

Contents lists available at ScienceDirect

Journal of Photochemistry and Photobiology A: Chemistry

journal homepage: www.elsevier.com/locate/jphotochem

Carbazole donor and carbazole or bithiophene bridged sensitizers for dye-sensitized solar cells

Anthony C. Onicha, Krishna Panthi, Thomas H. Kinstle, Felix N. Castellano*

Center for Photochemical Sciences and Department of Chemistry, Bowling Green State University, Bowling Green, OH 43403, USA

ARTICLE INFO

Article history:
Received 4 April 2011
Received in revised form 15 June 2011
Accepted 1 August 2011
Available online 9 August 2011

Keywords:
Organic DSSC
Carbazole donor
Carbazole linker
Photochemically stable organic sensitizer

ABSTRACT

Three metal-free organic sensitizers consisting of carbazole as an electron donor, carbazole or bithiophene as the linker and cyanoacrylic acid as the electron acceptor and anchoring groups were designed and synthesized for use in dye-sensitized solar cells (DSSCs). The sensitizers were characterized by ^{1}H and ^{13}C NMR, MALDI-TOF (or HRMS), UV–Vis, photoluminescence, and electrochemistry. The HOMO and LUMO electron distributions of the sensitizers were calculated using density functional theory on a B3LYP level for geometry optimization. The photovoltaic performance of the sensitizers in operational liquid junction-based DSSCs under AM 1.5 G one-sun excitation (100 mW/cm^2) indicate that the sensitizers are promising candidates for use in DSSCs. Sensitizers **1** and **2** produce a power conversion efficiency of 2.70% with a maximum IPCE of 75% at 450 nm, while sensitizer **3** has a power conversion efficiency of 2.23% with a maximum IPCE of 66% at 440 nm. The sensitizers thus exhibit excellent photon-to-current conversion efficiencies in the blue region of the spectrum and serve as candidates for further strategic optimization in tandem cells.

1. Introduction

Dye-sensitized solar cells (DSSCs) have been attracting a great deal of interest due to the potential of high energy conversion efficiency at low cost [1,2]. Since the original breakthrough in DSSCs [1,3], ruthenium polypyridyl complexes have been widely used as sensitizers in DSSCs, and the highest reported NREL-certified power conversion efficiency of 11.18% has been obtained for the **N719** sensitizer, a derivative of *cis*-Ru(dcbpyH$_2$)(NCS)$_2$ (the **N3** sensitizer) [4]. In addition to ruthenium polypyridine sensitizers, other organometallic sensitizers such as osmium(II) polypyridine sensitizers [5–7], platinum(II) sensitizers [8], and zinc(II) sensitizers [9,10], amongst others, have also been investigated by researchers. Although the metal-complexed sensitizers exhibit high efficiency and stability, they are expensive and difficult to purify compared to the metal-free organic sensitizers. Metal-free organic sensitizers also show promise due to advantages such as low cost, high molar extinction coefficient, and facile molecular design. Recently, an unprecedented power conversion efficiency of 10.3% was reported for an organic sensitizer [11], thus indicating that with further strategic optimization, metal-free organic sensitizers may overtake their organometallic counterparts in photovoltaic performance.

Novel organic sensitizers such as coumarin [12–14], tetrahydroquinoline [15,16], merocyanine [17,18], cyanine [19,20], phenothiazine [21], indoline [22,23], and hemicyanine [24,25] have been used in DSSCs with good results. Still, a more strategic molecular design of organic sensitizers is required to achieve higher efficiency (η) values. The requirements [17,24,26] of efficient sensitizers for use in DSSCs include (a) wide absorption range and high absorption coefficient that give high light harvesting efficiency, (b) excited-state redox potential should match the energy of the conduction band, (c) light excitation associated with vectorial electron flow from the light-harvesting moiety of the sensitizer towards the surface of the semiconductor, (d) conjugation across the donor and the anchoring group, (e) good anchoring group and, (f) electronic coupling between the lowest unoccupied molecular orbital (LUMO) of the sensitizer and the TiO_2 conduction band. The major factors that result in low conversion efficiency of many organic sensitizers in the DSSCs are (a) the aggregation of sensitizer on the semiconductor surface and (b) recombination of conduction-band electrons with the iodide/triiodide redox mediator [27]. Many metal-free organic sensitizers usually exhibit excellent incident photon-to-current efficiency in the blue region of the spectrum with little or no photoaction in the lower energy regions [28,29]. A tendency to π-stack exists in π-conjugated planar molecules due to strong intermolecular interactions between π-electrons and may result in a dissipative intermolecular energy transfer which could have adverse effects on the photovoltaic performance of DSSCs incorporating these types of molecules [30,31].

* Corresponding author. Tel.: +1 419 372 7513; fax: +1 419 372 9809.
E-mail addresses: castell@bgsu.edu, castell@bgnet.bgsu.edu (F.N. Castellano).

1010-6030/$ – see front matter © 2011 Elsevier B.V. All rights reserved.
doi:10.1016/j.jphotochem.2011.08.001

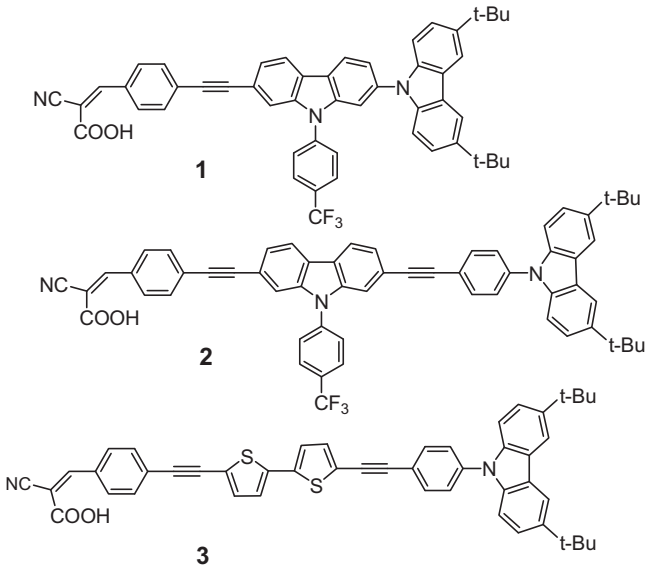

Fig. 1. Chemical structures of the sensitizers **1**–**3**.

Minimization of the extent of aggregation of organic sensitizers and charge recombination through appropriate structural modification becomes necessary in order to achieve optimal performance. On the basis of these strategies, we have designed and synthesized organic dyes for use as sensitizers of DSSCs. The very few organic compounds incorporating carbazole [32–34] which have been used as sensitizers in DSSCs exhibit exciting results. Also, a few reports on sensitizers incorporating thiophene-based spacers and exhibiting good device efficiencies have appeared [35]. To date, there are no reports related to sensitizers bearing the carbazole moiety, in which it functions as both the donor and the linker. Therefore, we are developing and evaluating the potential of compounds bearing carbazole donor and carbazole or thiophene linker as sensitizers in organic solar cells. Carbazole-based sensitizers have been shown to exhibit excellent photovoltaic characteristics in the blue region of the spectrum [33,34]. These sensitizers may eventually be mixed with other sensitizers that exhibit excellent photovoltaic responses in the red in a tandem cell. This sort of tandem arrangement becomes necessary since extending the spectral response of individual sensitizers to low energy regions of the spectrum will ultimately result in ground and excited states that are not thermodynamically well aligned for sensitizer regeneration and electron injection. Also, we are interested in an excellent hole-transporting material such as carbazole moiety, and solid-state DSSCs [29,36].

In this article we report the design and synthesis of (2-cyano-3-[4-((3′,6′-di-*tert*-butyl-9-[4-(trifluoromethyl)phenyl]-9*H*-2,9′-bicarbazol-7yl)ethynyl)phenyl]acrylic acid) (**1**) and (2-cyano-3-(4-(2-(5-(2-(4-(3,6-di-*tert*-butyl-9*H*-carbazolyl)phenyl)ethynyl)-2,2′-bithiophene)ethynyl)phenyl)acrylic acid) (**3**) that exhibit maximum photovoltaic performance in the blue region of the spectrum. The design and synthesis of sensitizer **2** is reported in our previous paper [37]. DSSCs using these carbazole-based sensitizers (**1**–**3**) are discussed herein. The chemical structures of these sensitizers are shown in Fig. 1. All the sensitizers have the same acceptor cyanoacrylic acid, which incorporates the carboxylic acid anchoring group, and identical carbazole donor but differ in the linker. Sensitizers **1** and **2** have 2-, 7-, 9-substituted carbazole linker and the sensitizer **3** has bithiophene group as a linker. Cyanoacrylic acid has evolved as the acceptor group of choice in metal-free organic sensitizers since it functions both as an electron acceptor and as an anchoring group and has been shown to outperform the carboxylic acid group in these roles [38].

2. Experimental

2.1. General

Triphenylphosphine, 5,5′-dibromo-2,2′-bithiophene, CuI, N,N-diisopropylethylamine, Na_2SO_4, $NaHCO_3$, CS_2CO_3, $PdCl_2(PPh_3)_2$, cyanoacetic acid, and ammonium acetate were purchased from Sigma Aldrich. Lithium iodide, 4-*tert*-butylpyridine (4-*t*Bupy), iodine and 1-*n*-propyl-3-methylimidazolium iodide (PMII) were available from our previous study [7]. 3,6-Di-*tert*-butylcarbazole, and 3,6-di-*tert*-butyl-9-(4-ethynylphenyl)-9H-carbazole were synthesized following the reported literature procedure [39]. The synthesis of sensitizers **1**, **3** and their precursors **7**, **9** and **10** is described here. The synthesis of sensitizer **2**, and the precursors **4**–**6** is described elsewhere [37,40]. Relevant structural characterization spectra (^{1}H and ^{13}C NMR) for compounds **1**, **3**, **7**, **9** and **10** are given in Supporting information.

2.2. Characterization, physical measurements and instrumentation

^{1}H and ^{13}C NMR spectra were measured on a Bruker 500 MHz spectrometer internally referenced to TMS. UV–Vis absorption spectra were measured on a Shimadzu UV-2401 spectrophotometer and photoluminescence spectra were recorded on Jobin-Yvon-Fluorolog-3 spectrometer. Electrochemical data were obtained using a BAS Epsilon electrochemistry workstation with a conventional three-electrode arrangement. Cyclic voltammetry measurements were carried out in either anhydrous acetonitrile or dichloromethane solution containing 0.1 M tetrabutylammonium hexafluorophosphate as the supporting electrolyte, a gold microdisk (1.6 mm diameter) working electrode (BAS model MF-2014), a platinum wire auxiliary electrode (BAS model MW-4130) and a Ag/AgCl (3 M NaCl) reference electrode (BAS model MF-2079), respectively. Measurements were conducted in *ca.* 1 mM electroactive substrate in an argon gas atmosphere with a scan rate of 300 mV/s and ferrocene was used as internal standard. For all measurements, potentials were recorded vs the ferrocenium/ferrocene (Fc^+/Fc^0) internal standard, and finally converted to $E_{1/2}$ vs the normal hydrogen electrode (NHE) using $E_{1/2}(Fc^+/Fc^0) = +0.69$ V vs NHE [41]. Incident photon-to-current conversion efficiency (IPCE) measurements were carried out using an instrument from PV Measurements, Inc., equipped with a xenon arc lamp and calibrated with a silicon reference photodiode. Current–voltage characteristics were measured on an *I*–*V* data acquisition system (PV Measurements, Inc.) equipped with a small area solar simulator (AM 1.5 Global) and an NREL-certified silicon reference solar cell (PVM 274, PV Measurements, Inc.) for calibrating the intensity of the simulated sunlight to 100 mW/cm^2, with the measured photocurrent being within 2% of its calibration value. Photocurrent density (J_{SC}) values directly measured using *I*–*V* curves were typically comparable to those estimated from the integrated EQE (IPCE) spectra. Estimation of J_{SC} was performed by the *I*–*V* software (PV Measurements Inc.) according to the ASTM standard E1021. The sandwiched solar cells were illuminated directly through the transparent conductive glass support containing the TiO_2 photoanode. The photovoltaic characteristics reported herein are overall yields that were not corrected for losses due to light absorption and reflection by the conductive glass substrate.

2.3. Synthesis and characterization

2.3.1. 4-((3′,6′-Di-tert-butyl-9-[4-(trifluoromethyl)phenyl]-9H-2,9′-bicarbazol-7-yl)ethynyl)benzaldehyde (**7**)

To a solution of compound **6** (200 mg, 0.38 mmol) in dry toluene (30 ml) was added 3,6-di-*tert*-butylcarbazole (160 mg, 0.42 mmol). The $Pd(OAc)_2$ (3%), P(t-Bu)$_3$ 7% and Cs_2CO_3 (495 mg, 1.5 mmol) were also added and stirred under argon at 110 °C for about 24 h. The reaction mixture was then cooled to room temperature and toluene was removed completely under vacuum. The solid mixture was dissolved in tetrahydrofuran and unreacted Cs_2CO_3 was removed under gravity filtration. The organic residue was then purified by column chromatography (silica gel, 8% ethyl acetate in petroleum ether) to give the product (180 mg, 66%). ^{1}H NMR (500 MHz, $CDCl_3$): δ 1.50 (s, 18H), 7.36 (d, 2H), 7.48 (dd, 2H), 7.55 (dd, 1H), 7.61 (dd, 2H), 7.68 (s, 1H), 7.30 (d, 2H), 7.78 (d, 2H), 7.90 (d, 2H), 7.91 (d, 2H), 8.18 (d, 2H), 8.22 (d, 1H), 8.34 (d, 1H) and 10.05 (s, 1H). ^{13}C NMR (500 MHz, DMSO): δ 32.0, 34.8, 88.9, 94.4, 108.3, 109.0, 113.2, 116.4, 120.1, 120.3, 120.6, 121.9, 122.2, 123.4, 123.7, 124.8, 127.1, 127.2, 127.5, 127.6, 129.5, 129.6, 129.7, 132.0, 135.4, 139.5,140.8, 142.0, 143.0, and 191.4. HRMS EI$^+$ calculated for $C_{48}H_{39}ON_2F_3$ 716.30146, measured 716.30024.

2.3.2. 4-(2-(5-Bromo-2,2′-bithiophene)ethynyl)benzaldehyde (**9**)

5,5′-Dibromo-2,2′-bithiophene (**8**) (0.45 g, 1.38 mmol), $PdCl_2(PPh_3)_2$ (16 mg), CuI (12 mg), N,N-diisopropylethylamine (1 ml) and DMF (9 ml) were mixed together in 100 ml round bottom flask. Then argon was bubbled for 20 min. Ethylene benzaldehyde (0.1 g, 0.77 mmol) was added and stirred for 12–14 h at 80 °C under argon atmosphere. Then the reaction mixture was poured into distilled water and extracted with DCM. The extract was washed with 0.5 M HCl, then it was washed using saturated $NaHCO_3$ and distilled water. The solution was dried using anhydrous Na_2SO_4, followed by the addition of pentane (1/3 volume of DCM). The resultant solution was filtered using a Buckner funnel with a layer of silica pad. The filtrate was dried under vacuum. The crude product was purified by flash chromatography (silica gel, 30% DCM in hexane) to obtain pure compound (0.17 g, 65%). ^{1}H NMR (500 MHz, $CDCl_3$): δ 6.96 (d, 1H), 6.99 (d, 1H), 7.03 (d, 1H), 7.22 (d, 1H), 7.65 (d, 2H), 7.87 (d, 2H) and 10.03 (s, 1H). ^{13}C (500 MHz, $CDCl_3$): δ 86.5, 93.6, 120.1, 121.4, 123.0, 123.6, 129.0, 129.6, 130.0, 131.7, 133.7, 135.5, 137.9, 138.8 and 191.3. HRMS EI$^+$ calculated for $C_{17}H_9OS_2Br$ 371.92783, measured 371.92912.

2.3.3. 4-(2-(5-(2-(4-(3,6-Di-tert-butyl-9H-carbazolyl)phenyl)-ethynyl)-2,2′-bithiophene)ethynyl)benzaldehyde (**10**)

To a solution of compound **9** (100 mg, 0.269 mmol) in diisopropylethylamine (0.5 ml) and DMF (7 ml) was added 3,6-di-*tert*-butyl-9-(4-ethynylphenyl)-9H-carbazole (344 mg, 0.9 mmol). After the solution was degassed with argon for 30 min while stirring, $PdCl_2(PPh_3)_2$ (6.7 mg), CuI (5.1 g), and triphenylphosphine (8 mg) were added. The reaction was then stirred for 14 h at 80 °C under argon. The solvent was evaporated using vacuum and crude product was obtained. The product obtained was recrystallized from DCM and hexane to obtain the product (150 mg, 82%). ^{1}H NMR (500 MHz, $CDCl_3$): δ 1.5 (s, 18H), 7.17 (d, 1H), 7.18 (d, 1H), 7.27 (d, 1H), 7.28 (d, 1H), 7.42 (d, 2H), 7.50 (ds, 2H), 7.61 (d, 2H), 7.69 (d, 2H), 7.75 (d, 2H), 7.91 (d, 2H), 8.16 (d, 2H) and 10.08 (s, 1H). ^{13}C (500 MHz, $CDCl_3$): δ 31.0, 32.0, 76.6, 76.8, 77.0, 77.3, 83.1, 86.7, 93.9, 94.3, 109.2, 116.3, 120.9, 121.6, 122.6, 123.6, 123.8, 124.2, 124.4, 126.4, 129.0, 129.7, 131.8, 132.6, 133.1, 133.9, 135.5, 138.0, 138.5, 138.8, 139.2, 143.3 and 191.4. HRMS EI$^+$ calculated for $C_{45}H_{37}ONS_2$ 671.23167, measured 671.22981.

2.3.4. 2-Cyano-3-[4-((3′,6′-di-tert-butyl-9-[4-(trifluoromethyl)-phenyl]-9H-2,9′-bicarbazol-7-yl)ethynyl)-phenyl]acrylic acid (**1**)

To a round bottomed flask containing a mixture of compound **7** (100 mg, 0.14 mmol), cyanoacetic acid (11 mg, 0.14 mmol), and ammonium acetate (1 mg) was added acetic acid (5 ml). The mixture was heated at 120 °C for 6 h and allowed to cool to room temperature. The resulting solid was filtered and washed with distilled water, diethyl ether and methanol to give a bright orange solid (82%). Mass spectrum (MALDI-TOF) m/z M$^+$ = 783. ^{1}H NMR (500 MHz, DMSO): δ 1.40 (s, 18H), 7.38 (d, 2H), 7.47 (dd, 2H), 7.59 (dd, 1H), 7.61 (s, 1H), 7.64 (dd, 1H), 7.10 (s, 1H), 7.90 (d, 2H), 8.40 (s, 4H), 8.10 (d, 2H), 8.30 (d, 2H), 8.38 (s, 1H), 8.47 (d, 1H) and 8.59 (d, 1H). ^{13}C NMR (DMSO): δ 32.3, 35.0, 89.7, 94.5, 108.3, 109.6, 113.5, 117.2, 119.9, 121.9, 122.1, 123.1, 123.3, 124.0, 124.2, 125.6, 127.2, 128.0, 128.1, 131.3, 132.5, 136.9, 139.3, 140.7, 141.8, 143.0, 153.5 and 163.6.

2.3.5. 2-Cyano-3-(4-(2-(5-(2-(4-(3,6-di-tert-butyl-9H-carbazolyl)phenyl)ethynyl)-2,2′-bithiophene)-ethynyl)phenyl)acrylic acid (**3**)

To a round bottomed flask containing a mixture of compound **10** (150 mg, 0.22 mmol), cyanoacetic acid (9 mg), and ammonium acetate (1 mg) was added acetic acid (10 ml). The mixture was heated at 120 °C for 8 h and allowed to cool to room temperature. The resulting solid was filtered and washed with distilled water, diethyl ether and methanol to give a bright red solid (142 mg, 86%). Mass spectrum (MALDI-TOF) m/z M$^+$ = 738. ^{1}H NMR (500 MHz, DMSO): δ 1.43 (s, 18H), 7.40 (d, 2H), 7.47–7.54 (m, 6H), 7.71 (d, 2H), 7.75 (d, 2H), 7.84 (d, 2H), 8.07 (d, 2H), 8.29 (s, 1H) and 8.1 (s, 2H). ^{13}C NMR (500, DMSO): δ 31.2, 32.3, 83.4, 86.2, 94.8, 109.7, 117.3, 120.3, 121.2, 122.0, 123.6, 124.3, 126.1, 126.2, 126.6, 131.2, 132.2, 133.5, 134.8, 135.5, 137.7, 138.4, 138.5, 138.6, 143.5 and 163.6.

2.4. Preparation of nanocrystalline TiO_2 electrode and transparent platinum cathode

The sol–gel synthesis of the colloidal TiO_2 paste has been described in detail elsewhere [7,42]. The prepared TiO_2 paste was doctor-bladed onto the conductive glass substrate (Hartford Glass, TEC-15) to give the transparent layer of TiO_2 film with a typical thickness of 13 μm. The obtained nanoparticle film was then dried at 125 °C for 6 min and a 5 μm thick scattering layer of mesoscopic TiO_2 (Solaronix, Ti-Nanoxide 300) was doctor-bladed on top of it. The resulting TiO_2 films were subsequently annealed for 30 min at 500 °C under oxygen flow in a tube furnace with ramped heating control of 5 °C per minute. Upon cooling to 100 °C, TiO_2 electrodes were immersed in 0.5 mM sensitizer solution in acetonitrile/*tert*-butanol (50:50, v/v, %) for 48 h at RT. Due to solubility limitations, sensitization of sensitizer **3** was carried out in THF solution. Transparent platinum-coated FTO cathodes were prepared as described elsewhere [7].

2.5. Sandwiched solar cell assembly

The active device area of the sensitized TiO_2 photoanode was adjusted to 0.25 cm^2. Stretched Parafilm-M was used as a spacer between the photoanode and the platinum counter electrode. The typical thickness of the spacer was 20–30 μm. A few drops of the redox electrolyte were placed on top of the active electrode area and a platinized FTO-glass counter electrode was placed on top. The electrodes were then sealed together using binder clips. For these studies, the redox electrolyte solution consisted of 0.2 M LiI, 0.05 M I_2, 0.7 M PMII and 0.5 M 4-*t*Bupy in anhydrous acetonitrile [43].

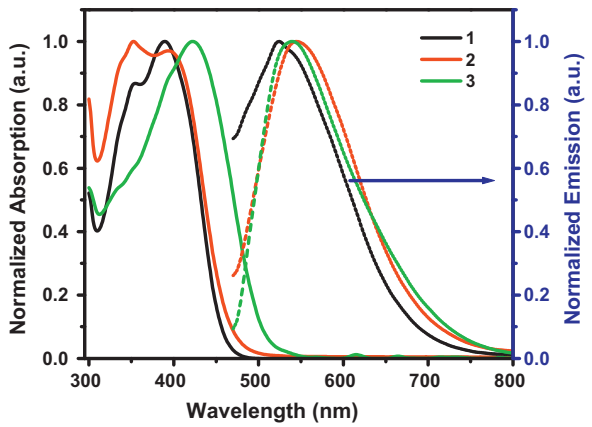

Fig. 2. Absorption–emission spectra of sensitizers **1**–**3** in dichloromethane.

3. Results and discussion

3.1. Synthesis and characterization

The preparation of 2,7-functionalized carbazoles is not straightforward, since both the 2- and 7-positions are in the meta position of the amino group of the carbazole unit and cannot be directly functionalized by standard electrophilic aromatic substitution. Successful synthetic strategies usually require functionalized 4,4′-biphenyl precursors with an additional reactive group at the 2 position used for a subsequent ring closure reaction. In this way 4,4′-biphenyl compound was converted into 2,7-dibromocarbazole (**4**) following a literature procedure [40]. N-arylation of **4** was followed by the Sonogashira coupling with 4-ethynylbenzaldehyde to obtain **6** (Scheme 1). Compound **6** reacts with 3,6-di-*tert*-butylcarbazole in presence of $Pd(OAc)_2$, $P(t\text{-}Bu)_3$ and Cs_2CO_3 to obtain **7** which further reacts with cyanoacetic acid, ammonium acetate and acetic acid to give the sensitizer **1**. On the other hand 5,5′-dibromo-2,2′-bithiophene (**8**) was converted into compound **9** by the Sonogashira coupling with 4-ethynylbenzaldehyde which further undergoes Sonogashira coupling with 3,6-di-*tert*-butyl-9-(4-ethynylphenyl)-9H-carbazole to obtain compound **10**. Compound **10** reacts with cyanoacetic, ammonium acetate and acetic acid to give the sensitizer **3**.

Reagents and conditions: (a) 1-bromo-4-trifluoromethylbenzene, K_2CO_3, DMF, reflux 12 h; (b) $Pd(PPh_3)_2Cl_2$, CuI, PPh_3, N,N-diisopropylethylamine, reflux 10 h; (c) $Pd(OAc)_2$ $P(t\text{-}Bu)_3$, Cs_2CO_3, toluene, reflux 22 h; (d) cyanoacetic acid, ammonium acetate, CH_3COOH, reflux 5 h; (e) $Pd(PPh_3)_2Cl_2$, CuI, PPh_3, N,N-diisopropylethylamine/DMF, reflux 14 h; (f) $Pd(PPh_3)_2Cl_2$, CuI, PPh_3, N,N-diisopropylethylamine, reflux 10 h; (g) cyanoacetic acid, ammonium acetate, CH_3COOH, reflux 5 h.

3.2. Photophysical properties

These sensitizers (**1**–**3**) are soluble in common organic solvents, such as dichloromethane (DCM), tetrahydrofuran (THF), dimethylformamide (DMF), and dimethylsulfoxide (DMSO). The absorption spectra of the sensitizers in DCM are shown in Fig. 2. All sensitizers have a strong absorption in the ultraviolet and blue regions with a maxima at 290 nm and around 350–430 nm, respectively. The absorption maxima at around 290 (not shown) are due to carbazole moiety and assigned to a π–π^* transition while the bands at around 350–430 nm are due to intramolecular charge transfer (ICT) between the donor carbazole and the acceptor moiety. A summary of photophysical properties of sensitizers **1**–**3** is given in Table 1. The minimum energy between the ground and excited states ($E_{0\text{-}0}$) was estimated as half the sum of the absorption and emission maxima, and the obtained value was subsequently converted to electron volts (eV). The excited state potential (E_{LUMO}) was determined as described elsewhere [7].

These sensitizers are composed of three main parts: a carbazole donor, a carbazole or bithiophene as a linker and cyanoacrylic acid as an acceptor and anchoring group. The donor groups may efficiently inhibit I_3^- from approaching the surface of the nanocrystalline TiO_2. The phenylethynyl spacer is a semi-rigid conjugated linker [44] which should favor the electron injection and the carbazole linker in sensitizers **1** and **2** can suppress the aggregation of dye molecules by the steric hindrance as trifluoromethyl benzyl group is attached at the 9H position of it.

3.3. Electrochemistry

The cyclic voltammogram of **1** in acetonitrile solution shows a quasi-reversible oxidation process centered at 1178 mV vs Ag/AgCl with the Fc^+/Fc^0 wave centered at 443 mV vs Ag/AgCl. The cyclic voltammogram of **2** in dichloromethane solution shows a quasi-reversible oxidation process centered at 1191 mV vs Ag/AgCl with the Fc^+/Fc^0 wave centered at 428 mV vs Ag/AgCl. Due to solubility limitations, the electrochemical properties of **3** could not be measured. Although sensitizer **3** has high solubility in tetrahydrofuran (THF), no oxidation waves were observed in THF solution within the solvent's potential window [45]. The oxidation potentials were further converted to $E_{1/2}$ vs NHE using $E_{1/2}(Fc^+/Fc^0) = +0.69$ vs NHE [41] yielding $E_{1/2}(\mathbf{1}) = 1.43$ V vs NHE and $E_{1/2}(\mathbf{2}) = 1.45$ V vs NHE. The sensitizers have oxidation potentials that are more positive than that of the I^-/I_3^- redox mediator (0.4 V vs NHE) [46] which provide a thermodynamic driving force of 1.03–1.05 V for regeneration of the oxidized sensitizers by the iodide/triiodide redox mediator. The excited state oxidation potentials of the sensitizers (Table 1) are sufficiently more negative than the conduction band edge of TiO_2, which is −0.5 V vs NHE [47], providing a great amount of thermodynamic driving force for electron injection.

3.4. Photovoltaic measurements

The photoaction spectra and *I*–*V* curves were measured under identical conditions for all the sensitizers investigated herein. Four independent DSSCs were assembled and measured in parallel and the results reported herein are the average of the four cells, represented as overall yields that were not corrected for any kind of losses. All devices have an active area of 0.25 cm^2. The photoaction spectra of dye-sensitized solar cells incorporating sensitizers **1**–**3**, along with that of the **N3** sensitizer, are presented in Fig. 3. The carbazole-based sensitizers convert visible light to photocurrent efficiently across the higher energy region over the wavelength range of 350–550 nm. A maximum photon-to-current conversion efficiency of about 75.1% at 450 nm was realized for sensitizers **1** and **2**, while sensitizer **3** has a maximum IPCE of 66.5 ± 0.64% at 440 (Fig. 3 and Table 2). The current–voltage properties of the DSSCs based on sensitizers **1**–**3**, as well as the **N3** sensitizer, measured under standard one-sun conditions (AM 1.5 G, 100 mW/cm^2) are shown in Fig. 4. Devices based on the carbazole-linked sensitizers **1** and **2** displayed the highest power conversion efficiency of about 2.7%, those based on the thiophene-linked sensitizer **2** displayed a power conversion efficiency of 2.23 ± 0.04%. Importantly, DSSCs based on these metal-free organic sensitizers displayed excellent fill factors which suggests that there is reduced contribution to the internal resistance within these devices, especially from the charge transport at the TiO_2/dye/electrolyte interface [48,49]. Compared with sensitizers **1** and **2**, sensitizer **3** possesses a higher short-circuit

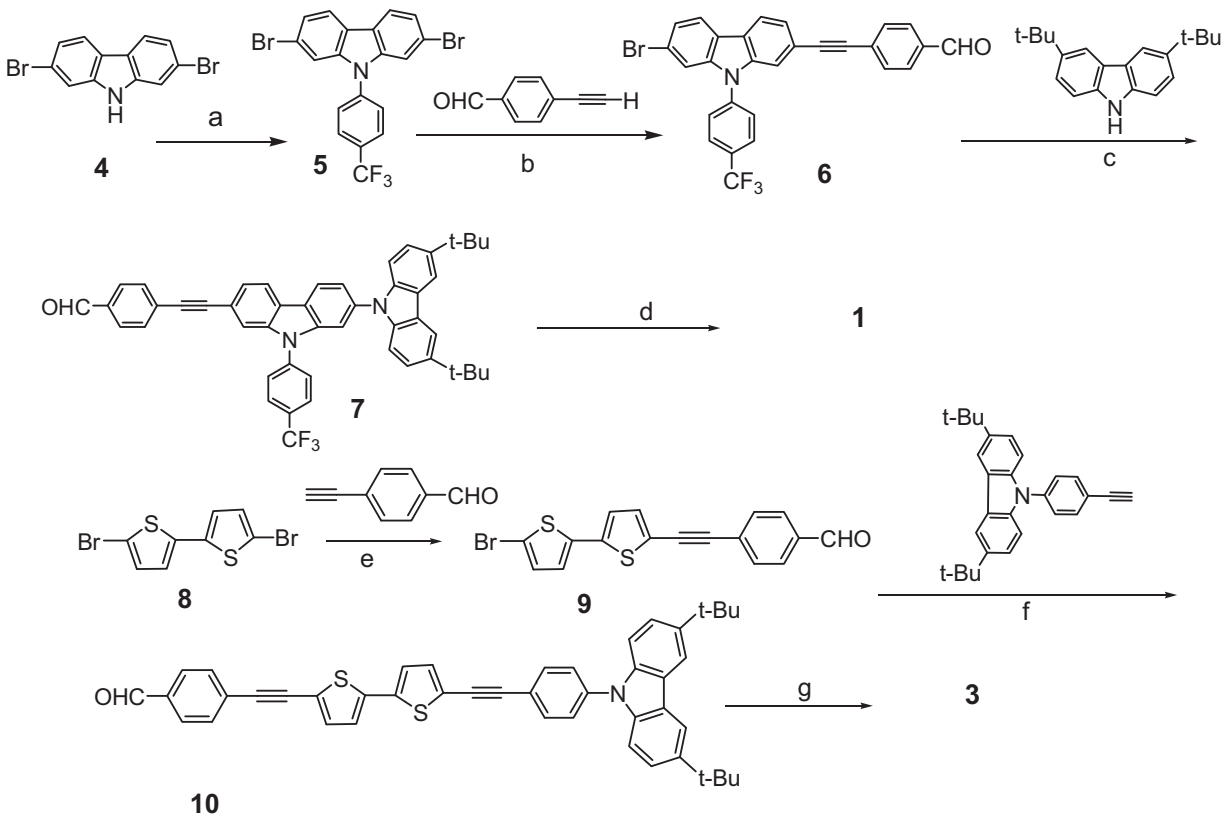

Scheme 1. Synthesis of sensitizers **1** and **3**.

Table 1
Summary of photophysical properties of sensitizers **1**–**3**.

Sensitizer	λ_{abs} (nm) ($\varepsilon \times 10^{-3}$ M^{-1} cm^{-1})	E_{OX} (V vs NHE)	Estimated $E_{0\text{-}0}$ (eV)	E_{LUMO} (V vs NHE)	λ_{em} (nm)
1	350 (35.76), 395 (34.12)	1.43	2.71	−1.28	524
2	350 (48.43), 385 (54.74)	1.45	2.63	−1.18	545
3	350 (11.09), 420 (16.42)	–	2.58	–	540

current despite having a lower value for the maximum IPCE. This is probably due to the fact that the sensitizer has a much broader absorption spectrum whose contributions are expected to enhance the value of the photogenerated current. Sensitizers **1** and **2** are structurally similar, except for the inclusion of an extra phenylacetylene group in the motif of sensitizer **2**, and as such should display similar properties which are reflected in the photophysical, electrochemical and photovoltaic properties of the sensitizers. The photogenerated short-circuit current and the values of the IPCE maxima are identical, within experimental error, for both sensitizers and the observed differences are revealed in the open-circuit voltage. There is a ~25 mV increase in the value of the V_{OC} of sensitizer **1** relative to sensitizer **2** which can be attributed to the effects of an extended π-conjugated backbone which enhances charge separation between the carbazole donor and cyanoacrylic acceptor moieties, enhances electron injection and occupancy of the conduction band which raises the Fermi level and ultimately results in a greater open-circuit voltage.

Due to concerns about the photostability of organic sensitizers in DSSCs, light-soaking tests were performed over 1 h with sandwich DSSCs based on sensitizer **2** and the results (Fig. 5) indicate a stable photovoltaic performance of the solar cells within the period under review. We were limited to such a small irradiation time duration given the fact that we are unable to permanently

Table 2
Summary of the photovoltaic properties of sensitizers **1**–**3** with **N3** sensitizer included for comparison.

Sensitizer	TiO_2 film thickness[a] (μm)	V_{OC} (mV)	J_{SC} (mA/cm^2)	FF (%)	η (%)	$IPCE_{max}$ (%)
1	13 + 5	649 ± 4.83	5.60 ± 0.10	67.4 ± 2.89	2.45 ± 0.04	74.0 ± 0.39
	16	615 ± 11.7	5.77 ± 0.07	68.7 ± 0.50	2.44 ± 0.00	74.4 ± 0.68
	16 + 5	617 ± 1.80	6.24 ± 0.30	70.2 ± 1.77	2.70 ± 1.77	75.3 ± 0.36
2	13 + 5	664 ± 9.03	4.72 ± 0.39	71.5 ± 1.00	2.24 ± 0.25	75.1 ± 0.18
	16	636 ± 4.41	5.73 ± 0.39	67.4 ± 6.11	2.44 ± 0.07	74.0 ± 0.75
	16 + 5	642 ± 6.59	5.96 ± 0.20	70.5 ± 1.23	2.70 ± 0.05	75.9 ± 0.57
3	16 + 5	523 ± 10.1	7.03 ± 0.28	60.5 ± 0.30	2.23 ± 0.04	66.5 ± 0.64
N3	16 + 5	683 ± 4.09	15.9 ± 1.01	55.9 ± 1.58	6.04 ± 0.31	71.5 ± 0.37

[a] Thickness of the transparent layer was either 13 or 16 μm while the scattering layer is 5 μm thick. Four identical solar cells were prepared and evaluated in each case. The redox electrolyte consisted of 0.2 M LiI, 0.05 M I_2, 0.7 M PMII and 0.5 M tbupy in acetonitrile solution.

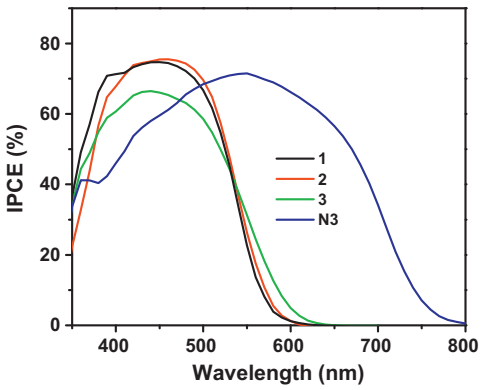

Fig. 3. Photoaction spectra of sensitizers **1**–**3** and **N3**. TiO_2 films consisted of a 16 μm transparent layer and a scattering layer is 5 μm thick. The redox electrolyte consisted of 0.2 M LiI, 0.05 M I_2, 0.7 M PMII and 0.5 M tbupy in acetonitrile solution.

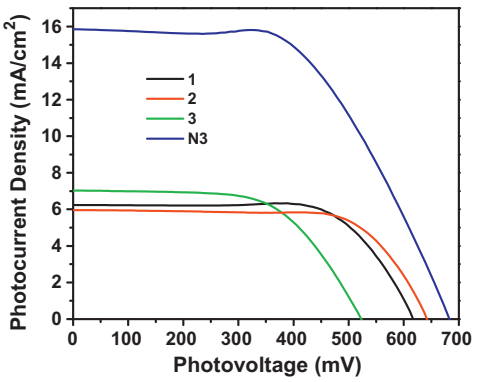

Fig. 4. Current–voltage curves of sensitizers **1**–**3** and **N3**. TiO_2 films consisted of a 16 μm transparent layer and a scattering layer is 5 μm thick. The redox electrolyte consisted of 0.2 M LiI, 0.05 M I_2, 0.7 M PMII and 0.5 M tbupy in acetonitrile solution.

seal the DSSCs. Apart from an initial (negligible) decrease in all the photovoltaic parameters in the first *ca.* 7 min, the performance indicators exhibited stable values and suggest that these sensitizers may withstand prolonged light-soaking. Prolonged light-soaking is usually accompanied by temperature increases which result in a faster rate of redox electrolyte diffusion and a downward shift in the conduction band edge potential relative to I^-/I_3^- [50]. The former results in improvements in fill factor and the latter in decreases in the open-circuit voltage, while observed increases in the short-circuit current are generally a combination of both effects. Similar experiments, performed at 50–55 °C over a 1000 h period, have been reported by Wang et al. [13] and it was shown that the power conversion efficiency and other photovoltaic properties stabilized over the period of the test, indicating that metal-free organic sensitizers exhibit adequate long term photostability, similar to the more frequently used coordination complex dye-sensitizers.

All photovoltaic performances were obtained with TiO_2 photoanodes incorporating 16 μm of a transparent layer and a 5 μm layer of scattering particles to yield the best photovoltaic performance (Table 2). Optimization of the TiO_2 film thickness is necessary in order to ascertain the optimum range that would yield the best photovoltaic performance and in this case involved the use of transparent layer of TiO_2 film (13 and 16 μm thickness) with or without a second layer of a 5 μm scattering layer on top of it (Table 2). Thicker films are expected to give better light absorption from an optical point of view since the films will adsorb more sensitizer molecules whose combined absorption properties will increase the light-harvesting property of the sensitized film. The thickness of a film affects its mechanical strength, adherence onto substrates and the interconnectivity between particles and these pose a challenge when making thicker films. Interconnectivity between particles is essential for efficient electron transport and influences resistance within the bulk semiconductor. Inefficient charge transport through the substrates results in losses through various recombination pathways. The optimal thickness of any given photoelectrode, on the other hand, depends on the extinction coefficient of the adsorbed sensitizer as well as on the semiconductor particle properties [51], and these conditions need to be optimized to realize the best performance for any given combination of semiconductor and sensitizer.

These sensitizers exhibit excellent photon-to-current conversion efficiencies in the blue region of the spectrum. Further work is focusing on developing metal-free sensitizers with excellent photoconversion efficiencies in the lower energy region and assembling the blue- and red-response sensitizers in a tandem arrangement to boost the energy conversion efficiency. The sensitizers reported herein exhibit unique photovoltaic behaviors and show promises for further optimization and application in the growing field of organic dye-sensitized solar cells.

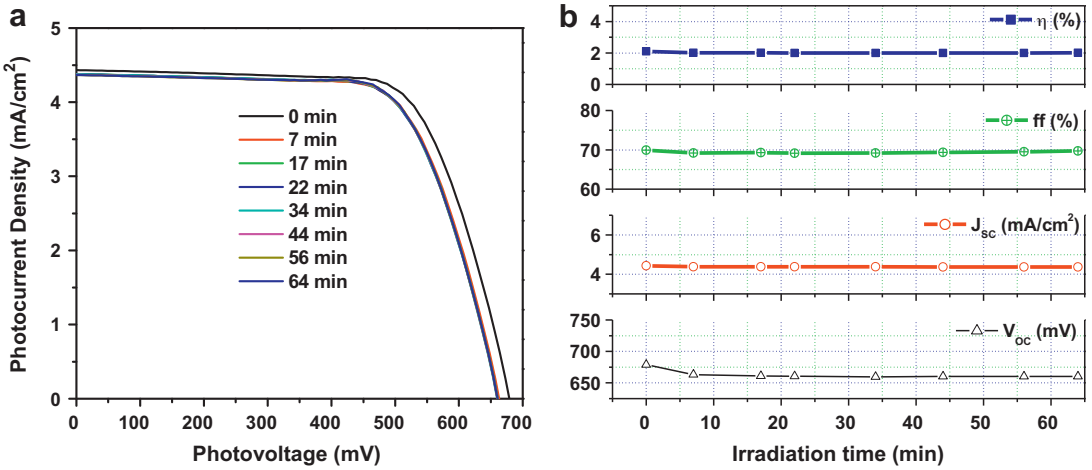

Fig. 5. Preliminary light-soaking test results for DSSCs based on sensitizer 2 showing (a) current–voltage curves and (b) properties of the current–voltage curves as a function of irradiation time.

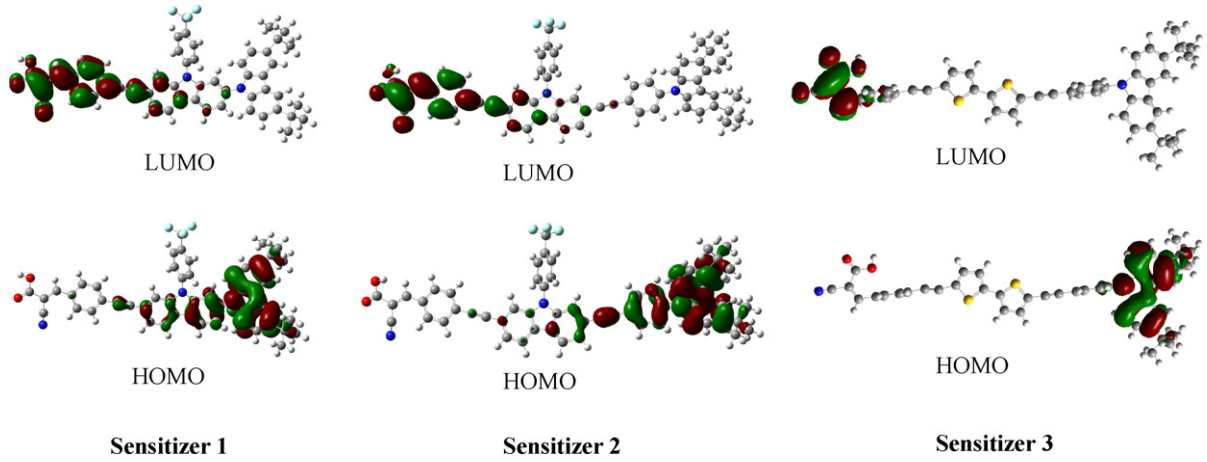

Fig. 6. HOMO–LUMO structures of the sensitizers **1**–**3** calculated using density functional theory.

3.5. Quantum chemical calculations

Density functional theory (DFT) calculations were performed on the sensitizers **1**–**3** to get a deep insight into the structure–photovoltaic cell performance relationships. The calculations were done on a B3LYP level for the geometry optimization. In the ground state, the electron density is localized mainly on the carbazole donor units, whereas in the excited state they move completely to the acceptor units near to the anchoring group, which favor the electron injection from the sensitizer to the conduction band of TiO_2. From the electron distribution structures in Fig. 6, it is obvious that the acceptor can withdraw almost all the electrons to the phenyl unit next to the anchoring group in all sensitizers **1**–**3**. The HOMO electrons are delocalized almost from donor carbazole to linker carbazole in sensitizer **1** but in sensitizer **2** it is not up to linker carbazole, whereas in sensitizer **3** the electrons are localized only in donor carbazole moiety. The absence of electronic communication between the thiophene linker and the donor carbazole in the HOMO on the one hand, and the linker and the acceptor cyanoacrylic acid on the other hand, in sensitizer **3** is closely related to the relatively higher energy of the linker, compared to the energies of the donor and acceptor groups. The electronic communication that exists in sensitizers **1** and **2** between the donor and the linker in the HOMO, and the acceptor and the linker in the LUMO, is made possible by the relative stabilization of the energy levels of the linker by the electron-withdrawing trifluoromethyl group. These theoretical results show that the sensitizers can have efficient electron injection from the LUMO to the conduction band of TiO_2 and improving the cell efficiency.

4. Conclusions

Organic sensitizers with a carbazole as a donor, carbazole or bithiophene as a π-conjugation linker and a cyanoacrylic acid group as an acceptor have been synthesized as for DSSCs. Compared with the sensitizer having bithiophene in the linker, the sensitizers containing carbazole linker showed more efficiency. Sensitizers **1** and **2** produce a power conversion efficiency of 2.70% with a maximum IPCE of 75% at 450 nm, while sensitizer **3** has a power conversion efficiency of 2.23% with a maximum IPCE of 66% at 440 nm. The sensitizers thus exhibit excellent photon-to-current conversion efficiencies in the blue region of the spectrum and serve as candidates for further optimization in tandem cells. These sensitizers could be mixed with other sensitizers with optimized red response in a tandem arrangement to achieve excellent photoconversion efficiencies in the spectral regions of interest. All the results indicate that these organic compounds are promising candidates in the development and further optimization of metal-free organic sensitizers for application in DSSCs.

Acknowledgements

We thank Gayani Wasana Pinnawala-Arachchilage for synthesis of sensitizer **3**. We also thank Dr. Ravi M. Adhikari for useful suggestions and Dr. Patrick Z. El-Khoury for quantum chemical calculations.

Appendix A. Supplementary data

Supplementary data associated with this article can be found, in the online version, at doi:10.1016/j.jphotochem.2011.08.001.

References

[1] B. O'Regan, M. Grätzel, Nature 353 (1991) 737.
[2] A. Hagfeldt, M. Grätzel, Acc. Chem. Res. 33 (2000) 269.
[3] N. Vlachopoulos, P. Liska, J. Augustynski, M. Grätzel, Am. Chem. Soc. 110 (1988) 1216.
[4] M.K. Nazeeruddin, F.D. Angelis, S. Fantacci, A. Selloni, G. Viscardi, P. Liska, S. Ito, B. Takeru, M. Grätzel, Am. Chem. Soc. 127 (2005) 16835.
[5] G. Sauve, M.E. Cass, G. Coia, S.J. Doig, I. Lauermann, K.E. Pomykal, N.S. Lewis, Phys. Chem. B 104 (2000) 6821.
[6] S. Altobello, R. Argazzi, S. Caramori, C. Contado, S.D. Fre, P. Rubino, C. Chone, G. Larramona, C.A. Bignozzi, Am. Chem. Soc. 127 (2005) 15342.
[7] A.C. Onicha, F.N. Castellano, Phys. Chem. C 114 (2010) 6831.
[8] A. Islam, H. Sugihara, K. Hara, L.P. Singh, R. Katoh, M. Yanagida, Y. Takahashi, S. Murata, H. Arakawa, Inorg. Chem. 40 (2001) 5371.
[9] W.M. Campbell, K.W. Jolley, P. Wagner, K. Wagner, P.J. Walsh, K.C. Gordon, L. Schmidt-Mende, M.K. Nazeeruddin, Q. Wang, M. Grätzel, D.L. Officer, Phys. Chem. C 111 (2007) 11760.
[10] L. Xiao, Y. Liu, Q. Xiu, L. Zhang, L. Guo, H. Zhang, C. Zhong, Tetrahedron 66 (2010) 2835–2842.
[11] W. Zeng, Y. Cao, Y. Bai, Y. Wang, Y. Shi, M. Zhang, F. Wang, C. Pan, P. Wang, Chem. Mater. 22 (2010) 1915.
[12] K. Hara, T. Sato, R. Katoh, A. Furube, Y. Ohga, A. Shinpo, S. Suga, K. Sayama, H. Sugihara, H. Arakawa, Phys. Chem. B 107 (2003) 597.
[13] Z.-S. Wang, Y. Cui, K. Hara, Y. Dan-oh, C. Kasada, A. Shinpo, Adv. Mater. 19 (2007) 1138.
[14] Z.-S. Wang, Y. Cui, Y. Dan-oh, C. Kasada, A. Shinpo, K. Hara, Phys. Chem. C 111 (2007) 7224.
[15] R. Chen, X. Yang, H. Tian, L. Sun, Photochem. Photobiol. A 189 (2007) 295.
[16] R. Chen, X. Yang, H. Tian, X. Wang, A. Hagfeldt, L. Sun, Chem. Mater. 19 (2007) 4007.
[17] K. Sayama, S. Tsukagoshi, K. Hara, Y. Ohga, A. Shinpou, Y. Abe, S. Suga, H. Arakawa, Phys. Chem. B 106 (2002) 1363.
[18] K. Sayama, K. Hara, N. Mori, M. Satsuki, S. Suga, S. Tsukagoshi, Y. Abe, H. Sugihara, H. Arakawa, Chem. Commun. 1173 (2000).
[19] W.-H. Zhan, W.-J. Wu, J.-l. Hua, Y.-H. Jing, F.-S. Meng, H. Tian, Tetrahedron Lett. 48 (2007) 2461.
[20] X. Ma, J. Hua, W. Wu, Y. Jin, F. Meng, W. Zhan, H. Tian, Tetrahedron 64 (2008) 345.

[21] H. Tian, X. Yang, R. Chen, Y. Pan, L. Li, A. Hagfeldt, L. Sun, Chem. Commun. 3741 (2007).
[22] T. Horiuchi, H. Miura, K. Sumioka, S. Uchida, Am. Chem. Soc. 126 (2004) 12218.
[23] L. Schmidt-Mende, U. Bach, R. Humphry-Baker, T. Horiuchi, H. Miura, S. Ito, S. Uchida, M. Grätzel, Adv. Mater. 17 (2005) 813.
[24] Z.-S. Wang, F.-Y. Li, C.-H. Huang, Phys. Chem. B 105 (2001) 9210.
[25] Y.-S. Chen, C. Li, Z.-H. Zeng, W.-B. Wang, X.-S. Wang, B.-W. Zhang, Mater. Chem. 15 (2005) 1654.
[26] K. Kalyanasundaram, M. Grätzel, Coord. Chem. Rev. 177 (1998) 347.
[27] D. Liu, R.W. Fessenden, G.L. Hug, P.V. Kamat, Phys. Chem. B 101 (1997) 2583.
[28] M.K.R. Fischer, S. Wenger, M. Wang, A. Mishra, S.M. Zakeeruddin, M. Grätzel, P. Bäuerle, Chem. Mater. 22 (2010) 1836.
[29] N. Ikeda, T. Miyasaka, Chem. Commun. 1886 (2005).
[30] Z.-S. Wang, N. Koumura, Y. Cui, M. Takahashi, H. Sekiguchi, A. Mori, T. Kubo, A. Furube, K. Hara, Chem. Mater. 20 (2008) 3993.
[31] X.-F. Wang, O. Kitao, H. Zhou, H. Tamiaki, S.-i. Sasaki, Phys. Chem. C 113 (2009) 7954.
[32] N. Koumura, Z.-S. Wang, S. Mori, M. Miyashita, E. Suzuki, K. Hara, Am. Chem. Soc. 128 (2006) 14256.
[33] D. Kim, J.K. Lee, S.O. Kang, J. Ko, Tetrahedron 63 (2007) 1913.
[34] C. Teng, X. Yang, C. Yuan, C. Li, R. Chen, H. Tian, S. Li, A. Hagfeldt, L. Sun, Org. Lett. 11 (2009) 5542.
[35] Y.-S. Yen, Y.-C. Hsu, J.T. Lin, C.-W. Chang, C.-P. Hsu, D.-J. Yin, Phys. Chem. C 112 (2008) 12557.
[36] M. Li, S. Tang, F. Shen, M. Liu, W. Xie, H. Xia, L. Liu, L. Tian, Z. Xie, P. Lu, M. Hanif, D. Lu, G. Cheng, Y. Ma, Chem. Commun. 3393 (2006).
[37] K. Panthi, R.M. Adhikari, T.H. Kinstle, Phys. Chem. A 114 (2010) 4550.
[38] J. Song, F. Zhang, C. Li, W. Liu, B. Li, Y. Huang, Z. Bo, Phys. Chem. C 113 (2009) 13391.
[39] Y. Liu, M. Nishiura, Y. Wang, Z. Hou, Am. Chem. Soc. 128 (2006) 5592.
[40] F. Dierschke, A.C. Grimsdale, K. Mullen, Synthesis (2003) 2470–2472.
[41] W.C. Barrette Jr., H.W. Johnson Jr., D.T. Sawyer, Anal. Chem. 56 (1984) 1890.
[42] S.-H.A. Lee, N.M. Abrams, P.G. Hoertz, G.D. Barber, L.I. Halaoui, T.E. Mallouk, Phys. Chem. B 112 (2008) 14415.
[43] S. Hwang, J.H. Lee, C. Park, H. Lee, C. Kim, C. Park, M.-H. Lee, W. Lee, J. Park, K. Kim, N.-G. Park, C. Kim, Chem. Commun. 4887 (2007).
[44] A.A. Bothner-By, J. Dadok, T.E. Johnson, J.S. Lindsey, Phys. Chem. 100 (1996) 17551.
[45] A.J. Bard, L.R. Faulkner, Electrochemical Methods Fundamentals and Applications, John Wiley & Sons Inc., New York, 1980.
[46] Z. Zhang, Z. Zhang, P. Chen, T.N. Murakami, S.M. Zakeeruddin, M. Grätzel, Adv. Funct. Mater. 18 (2008) 341.
[47] M. Grätzel, Inorg. Chem. 44 (2005) 6841.
[48] L. Han, N. Koide, Y. Chiba, T. Mitate, Appl. Phys. Lett. 84 (2004) 2433.
[49] L. Han, N. Koide, Y. Chiba, A. Islam, R. Komiya, N. Fuke, A. Fukui, R. Yamanaka, Appl. Phys. Lett. 86 (2005) 213501.
[50] B.C. O'Regan, J.R. Durrant, Phys. Chem. B 110 (2006) 8544.
[51] Z.-S. Wang, H. Kawauchi, T. Kashima, H. Arakawa, Coord. Chem. Rev. 248 (2004) 1381.